Article

From Sweet Sorghum to Sesquiterpene and Bio-Aviation Fuel: Production and EIA Analysis

Yunpeng Jia [1,†], Baoyin An [1,†], Jin Zhang [2], Yibing Kou [2], Huili Zhang [1,*,†], and Meng Wang [1,*,†]

[1] State Key Laboratory of Green Biomanufacturing, Beijing University of Chemical Technology, Beijing 100029, China
[2] Beijing Advanced Innovation Centre for Soft Matter Science and Engineering, Beijing University of Chemical Technology, Beijing 100029, China
* Correspondence: zhhl@mail.buct.edu.cn (H.Z.); wangmeng@mail.buct.edu.cn (M.W.)
† These authors contributed equally to this work.
Received: 21 November 2025; Revised: 8 December 2025; Accepted: 14 December 2025; Published: 22 December 2025

Abstract: The worldwide aviation industry is booming, but global aviation fuel emissions are increasing. The production of bio-aviation fuel is a worldwide hot topic. Sorghum, the world's fifth most important cereal crop after rice, wheat, maize, and barley, is a potential source of carbohydrates, and a potential candidate for the production of bio-aviation fuel after fermentation, intermediate (sesquiterpene) upgrading and polishing. The sweet sorghum agro-cycle reveals a yield of 60 t/ha of carbohydrate-rich straw with a carbohydrate content of 11–21%. All input materials and energy uses are determined. Mostly fermentation CO_2, fertilizers and transportation fuels contribute to the environmental impact. Full mass and energy balances are established through Aspen Plus V12 simulation. The EIA of the sorghum to "on flight" bio-aviation fuel is then assessed with CH_4, NO_x, SO_x and CO (from fuel combustion) contributing for over 80%. A sensitivity analysis confirms these high impacts, with the transportation distance mostly as dominant factor.

Keywords: sweet sorghum; fermentation; upgrading; sesquiterpene; intermediate; bio-aviation fuel; EIA

1. Introduction

1.1. The Need to Produce Bio-Aviation Fuel by Using Sustainable Feedstock and Energy

The worldwide aviation industry is booming, but global aviation fuel emissions are like an "environmental bomb" that is constantly exerting a negative impact on the climate. In order to deal with the problem of emission reduction, many solutions have emerged [1,2]. Among the solutions, bio-aviation fuels based on renewable energy and feedstock stand out and have significant advantages. Bio-aviation fuel can not only effectively reduce carbon emissions, but also has stable and reliable energy supply characteristics, in line with the sustainable development demands of the aviation industry. The demand for aviation fuel continues to grow, but fossil fuel remains the main available source for aviation fuel. According to a new report, the global demand for bio-aviation fuel was estimated at approximately 18 million tons per year (Mton/year) in 2020, and it is projected to increase to 44 million tons (Mton) by 2035. To date, 60 airlines have set specific targets for this fuel [3–5]. The development of renewable aviation fuels is of great significance to energy conservation and emission reduction and is a key strategy to promote the green transformation of the aviation industry, as endorsed worldwide.

When considering "green" energy, the use of solar—driven technology is a major focus. Towards a "green" feedstock, mainly biomass is currently considered [2], and within the target, sweet sorghum will be used as "green" feedstock. Hydrogen will play a key role, but can be produced by sustainable production methods [1,2,6,7].

1.2. Sweet Sorghum and Its Agro-Cycle

1.2.1. Sweet Sorghum

Sorghum bicolor, commonly called sorghum, and also known as great millet or milo, is a species in the grass genus Sorghum is cultivated for its grain, used for human food. The plant is used for animal feed and ethanol production. Sorghum originated in Africa, and is now cultivated widely in tropical and subtropical regions.

Sorghum is the world's fifth-most important cereal crop after rice, wheat, maize, and barley. Sorghum is typically annual, but some cultivars are perennial. The grain is small, 2 to 4 mm in diameter. Sweet sorghums are cultivars primarily grown for forage, syrup production, and ethanol.

Sorghum is closely related to maize and the millets within the PACMAD clade of grasses, and more distantly to the cereals of the BOP clade such as wheat and barley, as illustrated in Figure 1.

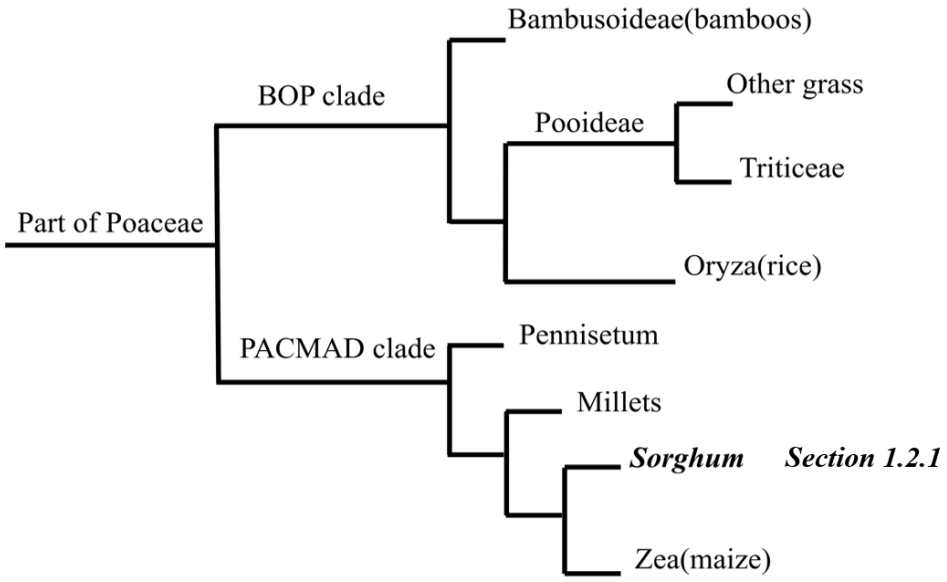

Figure 1. Grass clades.

Most varieties of sorghum are drought- and heat-tolerant, nitrogen-efficient, and are grown particularly in arid and semi-arid regions where the grain is one of the staples for poor and rural people. These varieties provide forage in many tropical regions. S. bicolor is a food crop in Africa, Central America, and South Asia. It is most often grown without application of fertilizers or other inputs by small-holder farmers in developing countries. They benefit from sorghum's ability to compete effectively with weeds, especially when planted in narrow rows. Sorghum actively suppresses weeds by producing sorgoleone, an alkylresorcinol.

Sorghum grows in a wide range of temperatures. The optimum growth temperature range is 12–34 °C (54–93 °F), and the growing season lasts for around 115–140 days. It can grow on a wide range of soils, such as heavy clay to sandy soils with the pH tolerance ranging from 5.0 to 8.5. It requires an arable field that has been left fallow for at least two years or where crop rotation with legumes has taken place in the previous year. It can recover growth after some drought. Diversified 2- or 4-year crop rotation can improve sorghum yield, additionally making it more resilient to inconsistent growth conditions. In terms of nutrient requirements, sorghum is comparable to other cereal grain crops with nitrogen, phosphorus, and potassium required for growth. For the storage requirements of sweet sorghum straw, in general, in the arid regions of northern China, most factories adopt a storage mode of sun-curing followed by baling and shed storage after straw harvesting. This approach can mitigate straw decomposition, reduce the risks of oxidative degradation of sugars and mold contamination in the straw, while featuring low cost and high applicability.

1.2.2. The Sweet Sorghum Agro-Cycle

According to the China Rural Statistical Yearbook [8], the average sorghum yield was determined to be 4.5 t/ha of sorghum grains and 60 t/ha of carbohydrate-rich straw. Sweet sorghum seeds can be used as grain. The carbohydrate content of sweet sorghum straw is 11–21%, and the brix of stem juice is 5–22%. The main components are sucrose, glucose and fructose. Sweet sorghum straw is squeezed to obtain sugar juice, which can be used for sesquiterpene fermentation by adding nutritional salts.

According to Jiang's [9] investigation, the amount of fertilizer applied, the amount of herbicide, lime, and pesticides applied during sweet sorghum planting, and the diesel consumption of agricultural machinery such as seeders and harvesters were determined.

The harvest period of sweet sorghum is half a month. After harvest, the sugar in the straw is easy to deteriorate and must be transported quickly to the processing site after harvest. Mature sweet sorghum will be processed into straw stacks by agricultural machinery such as grass grazers and mobile balers, and then transported to the factory

by small trucks or all-trailer trucks as soon as possible for subsequent pretreatment, fermentation and other processes. Specific information on agricultural machinery and transportation is as follows.

Based on the agricultural machinery information obtained from the investigation, a grass grabber with a fuel consumption of 2.5 L/t and a baler with a fuel consumption of 2.7 L/t are commonly used to process sweet sorghum straw. According to different actual conditions and geographical locations, Sun [10] conducted field investigations and found that the loading volume of straw was about 7 tons; Cao [11] proposed that there are three main types of straw transportation vehicles, namely flatbed trailer modified shape, double-door full trailer, and side-dump full trailer. Based on field observations and literature research, the straw loading volume was set to 10 tons and the single transportation mileage was set to 25 km.

The separation process of sweet sorghum sugar juice involves washing roughly with water spray, cutting and tearing, squeezing with a press, crude sugar juice vacuum concentration and concentrated sugar juice.

Water spray for rough washing uses the same amount of water as the straw. The Qufu Huachen Machinery Crop Straw Crusher is used for cutting and tearing, with a power of 4 kW and a single processing capacity of 3.8 t/h. A sugarcane press (Model TSG 318 × 408) with a production capacity of 1.25 t/h was employed for the squeezing process. The MVR evaporator with the evaporation capacity of 500 kg/h was used for vacuum concentration. The purpose of concentration was to extend the storage time. After completing the above process, storing sweet sorghum-derived glucose at room temperature, and the heating energy consumption of the heating coil is not calculated. The straw residue produced after crushing can be used as feed to cows, sheep and deer. The manure can be digested to produce biogas, used for lighting, cooking or passed into greenhouses to increase the yield of vegetables and flowers. The produced fertilizer can be returned to the field to improve the soil and protect the environment. Table 1 presents the mass and energy balances of the cycle.

Table 1. Agro-cycle mass and energy balance.

Stage	Input Raw Materials/ Energy Consumption	Value	Output Product	Value	Data Sources
S1 Sweet sorghum planting	N-fertilizer	211 kg/ha	Sweet sorghum seeds	4.5 t/ha	[9]
	P-fertilizer	63 kg/ha	Sweet sorghum straw	60 t/ha	
	K-fertilizer	54 kg/ha			
	Herbicide	5.kg/ha			
	Lime	94 kg/ha			
	Pesticides	0.75 kg/ha			
	Fuel oil	2211 MJ/ha			
S2 Straw collection and transportation	Transportation distance	25 km			[11]
	Quantity of transported straw	10 ton			
	Fuel oil	1716 MJ			
S3 Straw pretreatment	Sorghum straw	750 ton	Sugar	11.2 ton	[12]
	Electrical energy	77,463 MJ	Residue	738.8 ton	
	Water	750 ton			

1.3. Objective of the Research and Manuscript

(1) Assess the sorghum agro-cycle
(2) Among the more important processes, the fermentation production of sesquiterpenes and the refining of sesquiterpenes into aviation fuel, were simulated by Aspen Plus
(3) Evaluate the carbon emissions and environmental impact of the process
(4) Determine the environmental impact assessment (EIA) of both the sorghum agro-cycle and the production process
(5) Compare EIA results with current fossil fuel-based bio-aviation fuel

2. Designing the Sweet Sorghum to Bio-Aviation Fuel Process

2.1. Overview of the Production of Sesquiterpene from Sweet Sorghum

The fermentation of sweet sorghum-derived glucose to sesquiterpenes applies on genetically modified yeast together with salts, vitamins and other substances to build the strain's culture environment.

The fermentation broth is separated by extraction, centrifugation and stripping to obtain high purity sesquiterpene products. The fermentation process was scaled-up from 100 L fermentation, 5000 L fermentation and 40 m^3 fermentation, the first two stages of fermentation were the strain cultivation stages in order to obtain high activity and high density of yeast, and the last stage was the main sesquiterpene production stage. In Section 2.1,

the process simulation software Aspen Plus will be used to assess the process, specifying NRTL as the main physical method.

The refining process from sesquiterpenes to bio-aviation fuels requires hydrogenation, rearrangement, and rectification processes to finally produce high-purity alkyl diamondanes, which is an aviation fuel component with the molecular formula of $C_{15}H_{26}$. In Part 2.2, process simulation software Aspen Plus will be used to evaluate the process, using PENG-Robinson as the main physical property method.

2.2. The Process Details and its ASPEN Simulation of the Sesquiterpene Production

2.2.1. Process Overview: Glucose to Sesquiterpenes

The fermentation of glucose to sesquiterpenes is carried out using genetically modified yeast, with glucose as the main sugar source and inorganic salts, vitamins, trace elements and other substances added to build the culture environment of the strain. The fermentation broth is separated by extraction, centrifugation and stripping to obtain high purity sesquiterpene products. The fermentation process was scaled-up by 100 L fermentation, 5000 L fermentation and 40 m^3 fermentation. The first two stages of fermentation were the strain cultivation stages in order to obtain high activity and high density of yeast, and the last stage was the main sesquiterpene production stage. The process simulation software Aspen Plus was used to assess the process, specifying NRTL as the main physical method. The overall workflow of the fermentation process is illustrated in detail in Figure 2.

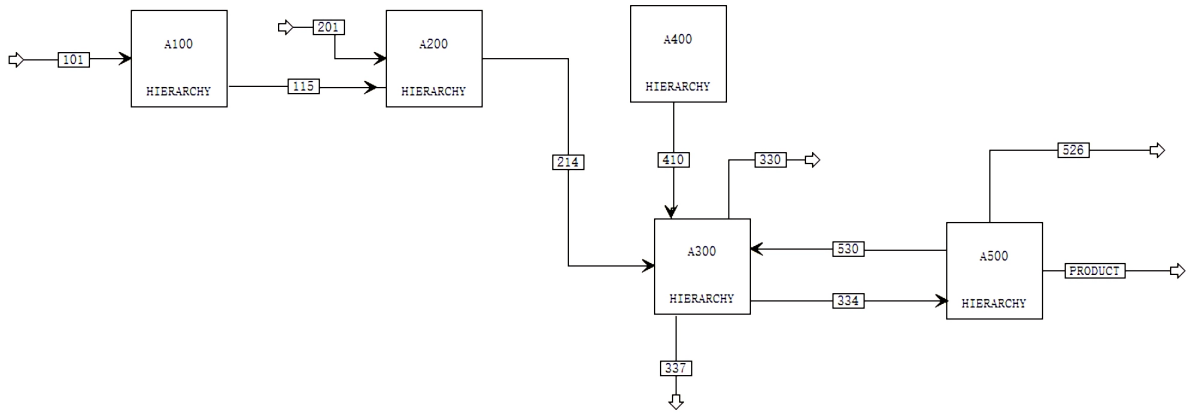

Figure 2. Flow chart of the total fermentation process (derived from simulation results).

2.2.2. Process Concept and Design

Fermentation and Amplification Section (Sub-Processes A100–A400)

Figures 3–6 illustrate the various stages of the simulated fermentation process. The initial yeast strain enters into the 100 L fermenter (sub-process A100), and the culture conditions are optimised under the experimental conditions to configure the culture solution with the best sugar source, inorganic salt, vitamins and trace elements. After autoclaving, the raw material is cooled to room temperature and put into a 100 L fermenter (RStoic module). The sterilisation equipment comprises a heater module, which works under 116 °C and atmospheric pressure. The operating condition of the fermenter is 30 °C and 0.08 MPa.

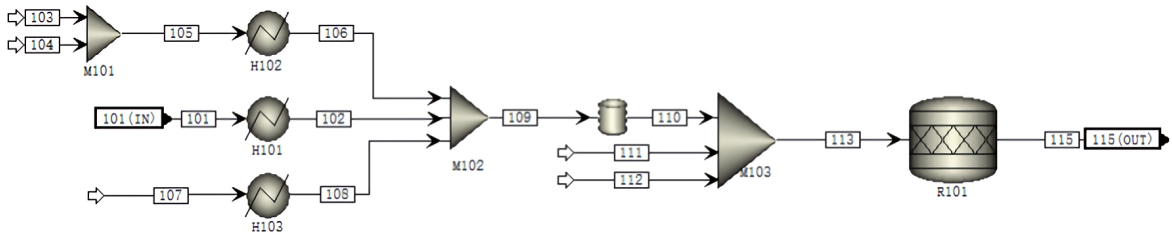

Figure 3. A100: Flow chart of 100 L fermentation (derived from simulation results).

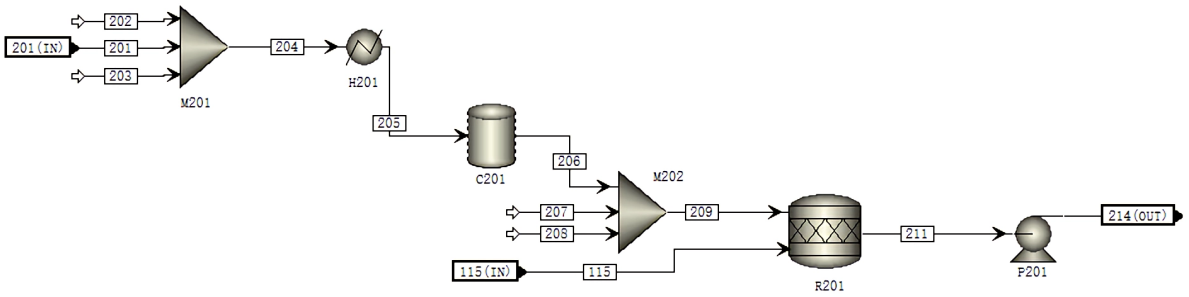

Figure 4. A200: Flow chart of 5000 L fermentation (derived from simulation results).

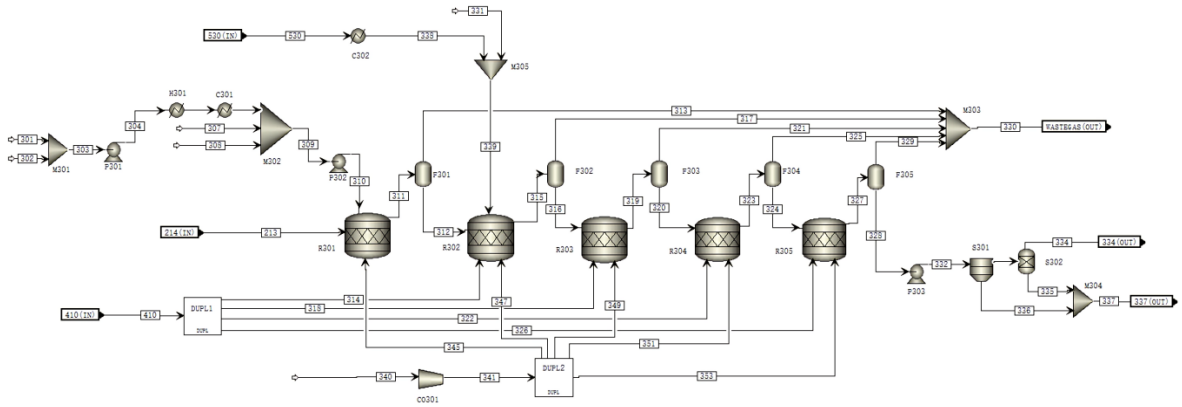

Figure 5. A300: Flow chart of 40 m^3 fermentation (derived from simulation results).

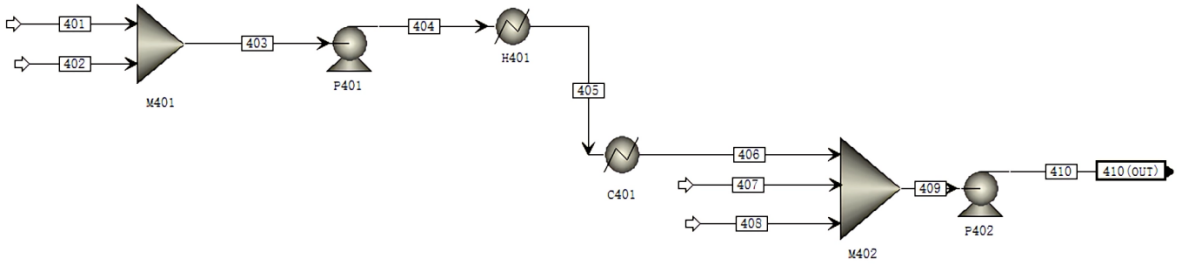

Figure 6. A400: Flow chart of 40 m^3 fermentation replenishment (derived from simulation results).

When the yeast in the tank reaches a suitable concentration, it is transferred to 5000 L fermenter for secondary culture (sub-process A200). 5000 L fermentation batching is also carried out under optimal conditions, and after autoclaving, it enters the fermenter. Unlike the 100 L fermenter, the 5000 L fermenter works at 0.025 MPa. The yeast reaches the right concentration, is transferred to the 40 m^3 fermenter and proceeds to the sesquiterpene fermentation stage (sub-process A300).

The 40 m^3 fermentation dosage is divided into feed and replenishment to meet the carbon source supplementation required for the growth and output of the yeast. The feed is consistent with the first two stages of the fermentation process. According to the fermentation scale increase year-by-year, the replenishment is mainly a sugar source supplementation; glucose accounted for an increase in the proportion of replenishment dosage in A400. In this stage of the fermentation process, the fermentation tank is still using the RStoic module, running at 30 °C, 0.025 MPa. According to the actual requirements, the replenishment is carried out four times, so that the simulation process used the five identical fermenters to represent the changes in the composition of the fermentation broth before and after recharging. The fermentation process was carried out under aerobic conditions, and the compressed air was fed into the fermenters at an appropriate injection rate (Compr module). In addition, poly α-olefins were added as extractants during the fermentation process to extract the produced sesquiterpenes into the organic phase for subsequent separation operations. Poly α-olefins were not present in the Aspen database and were replaced with hexacosane ($C_{60}H_{122}$) during the simulation.

After the addition of extractant, the fermentation broth is divided into three phases: organic, aqueous and solid, where the organic phase consists mainly of sesquiterpenes and poly α-olefins; the aqueous phase consists of water and unconsumed salts and other fermentation broth residues; and the solid phase consists mainly of bacterial

bodies. At the end of the fermentation, the fermentation broth was transported into a disc centrifuge (CFuge module) to separate the solids under conditions of 30 °C and 1.2 bar, under which 90% of the yeast was recovered. The liquids were extracted (Sep module) to obtain the upper organic phase, in which the recovery of the organic phase was set to be 100%, and the remaining aqueous phase was disposed of as a fermentation waste stream.

Stripping Section (Sub-Processes A500)

Details regarding the simulated stripping process are presented in Figure 7. After extraction and centrifugation to obtain a mixed stream of poly α-olefins and product sesquiterpenes, a nitrogen vapour stripping process was proposed to separate the sesquiterpenes in order to obtain a high purity sesquiterpene product. The organic phase is heated to 189 °C and fed from the top of the stripper tower (RadFrac module), while the nitrogen is heated to 200 °C and fed from the bottom of the tower. The stripper tower does not have an additional condenser or reboiler, and relies on the heat of the stream itself for material exchange, with the sesquiterpene product being carried out by nitrogen from the top of the tower, and polyalphaolefins with a high boiling point being the main product at the bottom of the tower. The vapour extraction tower was set up with 6 theoretical plates, and the convergence method was chosen to be 'very undesirable liquid phase', under which the recovery of sesquiterpenes at the top of the tower was up to 88.8%, with a large amount of sesquiterpenes still remaining in the extractant. In order to further recover the remaining sesquiterpene products, another identical stripper tower was set up for secondary separation. The primary stripper kettle distillate is heated from the top of the tower into the secondary stripper tower, and the heated nitrogen still enters from the bottom of the tower. The configuration of the two stripper towers is basically the same, and about 99.8% of the sesquiterpenes can be recovered by the separation of the two towers. The top stream of the stripper tower is flash evaporated to remove nitrogen, and then high purity sesquiterpene products can be obtained.

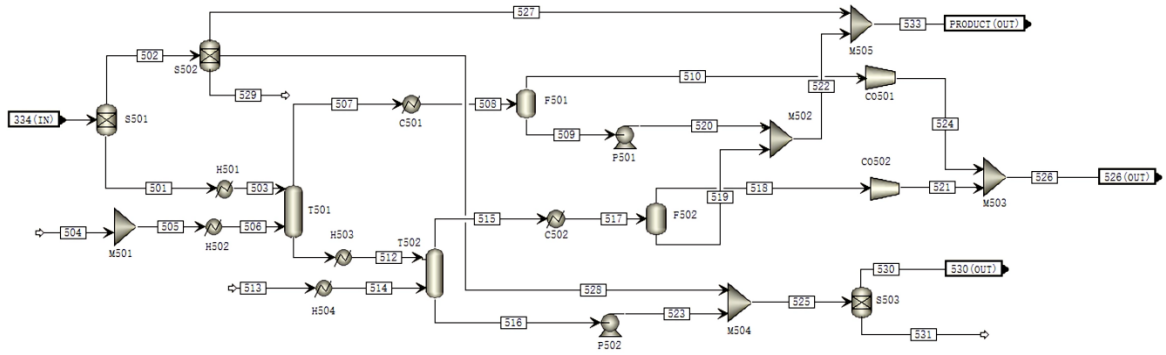

Figure 7. A500: Flow chart of stripping (derived from simulation results).

It should be noted that, according to the actual demand, the process uses three batches of the same fermentation process running at the same time (process is not shown), the amount of feed and discharge are corrected in this way. The fermentation process is an intermittent process, the fermentation cycle is about 168 h, while the separation process is in the form of a continuous vapour stripping, so that the vapour stripping process capacity is allocated according to the fermentation cycle.

2.2.3. Mass and Energy Balance

Material accountancy is the process of calculating the balance of materials in and out of a process. Aspen Plus can automatically generate the logistics information corresponding to each flow strand for the established process run calculations, and carry out material accountancy for the Sesquiterpene fermentation process based on these logistics data and the process scale. The results of the material balance of the sesquiterpene fermentation process are shown in Table 2.

As can be seen from Table 2, the imported material for the sesquiterpene fermentation process is 30,424 kg/batch, and a single batch of fermentation in a single fermenter yields 707 kg of product sesquiterpenes. With an annual operation of 8000 h as a basis for calculation, results in an annual yield of 101 t of sesquiterpene by fermentation under the conditions of three batches of the same fermentation.

In the above material accounting process, only the key logistics are collated, and factors such as aeration usage cannot be fully accounted for and are not involved in the accounting process. Fermentation process terminal fermentation liquid composition is complex, the content of unreacted raw materials is small and difficult to purify,

forced recovery will significantly reduce the economic benefits of the process. In the material control of this process, only the extractant material is separated and purified and recycled, and according to experimental calculations, the recovery rate of extractant can reach 80%.

Table 2. Sesquiterpene fermentation material balance.

Inputs	Mass Flow (kg/batch)	Outputs	Mass Flow (kg/batch)
Glucose	7178	Sesquiterpene	707
Water	22,228		
Inorganic salt	499	Recovered extractants	408
Vitamins	7.23	Waste liquids	24,486
Trace element	1.68	Waste gas	3199
Extractant (Poly α-olefins)	510	Recovered yeast	1624
Total	30,424	Total	30,424

In the simulation process, heat exchange facilities are used Heater module, and in the role of the appropriate utilities for the exchange of heat, the stream will be heated or cooled to the required temperature; process used in the stripping tower does not have an external condenser and heat exchanger, relying on the already heated logistics in the tower to complete the exchange of heat and material, so the stripping equipment has no energy input. The pressurisation of the liquid, gas logistics operation relies on pumps (Pump module) and compressors (Compr module), the energy input is electrical energy. The energy consumption of the process under the above provisions is summarised in Table S1.

According to Table S1, the process utilities mainly consist of cooling water, chilled brine, low pressure steam, high pressure steam, and electricity. The consumption of electricity accounts for a relatively small amount of energy due to the fact that the pumps and compressors in the process do not deliver a high pressure. Secondly, low pressure steam is used to heat the sterilisation facility, with a consumption of 26.9 kg/h of low pressure steam for the single batch fermentation process. The addition of chilled brine cools the top material of the stripper tower to a low temperature for efficient nitrogen removal to obtain a high purity sesquiterpene product, with a consumption of about 129 kg/h of chilled brine. The high temperature demand of the feed to the stripper was achieved by heat exchange with high pressure steam, which was used at a rate of 5.5 kg/h.

$$\mathrm{TEC} = \mathrm{THEC} + \mathrm{TCEC} \tag{1}$$

$$\mathrm{THEC} = \mathrm{M_{LP}} \times \mathrm{HV_{LP}} + \mathrm{M_{HP}} \times \mathrm{HV_{HP}} \tag{2}$$

$$\mathrm{TCEC} = \mathrm{M_{CW}} \times \mathrm{HV_{CW}} + \mathrm{M_{CB}} \times \mathrm{HV_{CB}} \tag{3}$$

The process energy consumption is summarised and calculated according to formulas (1)–(3), where TEC is the total energy consumption, THEC is the total heating energy consumption, TCEC is the total cooling energy consumption, M is the corresponding utility consumption, HV is the heating value, and CV is the cooling value. The total energy consumption of the process for the production of sesquiterpenes by glucose fermentation was 163.9 MJ/h, of which 97.1 MJ/h was used for heating and 66.8 MJ/h for cooling.

2.3. Sesquiterpene Refining into Bio-Aviation Fuel

2.3.1. Process Review

α-Longipinene is a typical sesquiterpene compound. After hydrogenation, saturated hydrocarbons are generated, and then trimethyl-ethyl-adamantane, pentamethyl-adamantane, ethyl-propyl-adamantane and some alkylcyclohexane and alkylnaphthalene by-products are obtained through rearrangement. Finally, alkyldiamondane aviation fuel products, by-products and recycled solvent 1,2-dichloroethane are obtained through rectification and separation. A feasible technological route for aviation fuel production using sesquiterpenes as the raw material is presented in Figure 8.

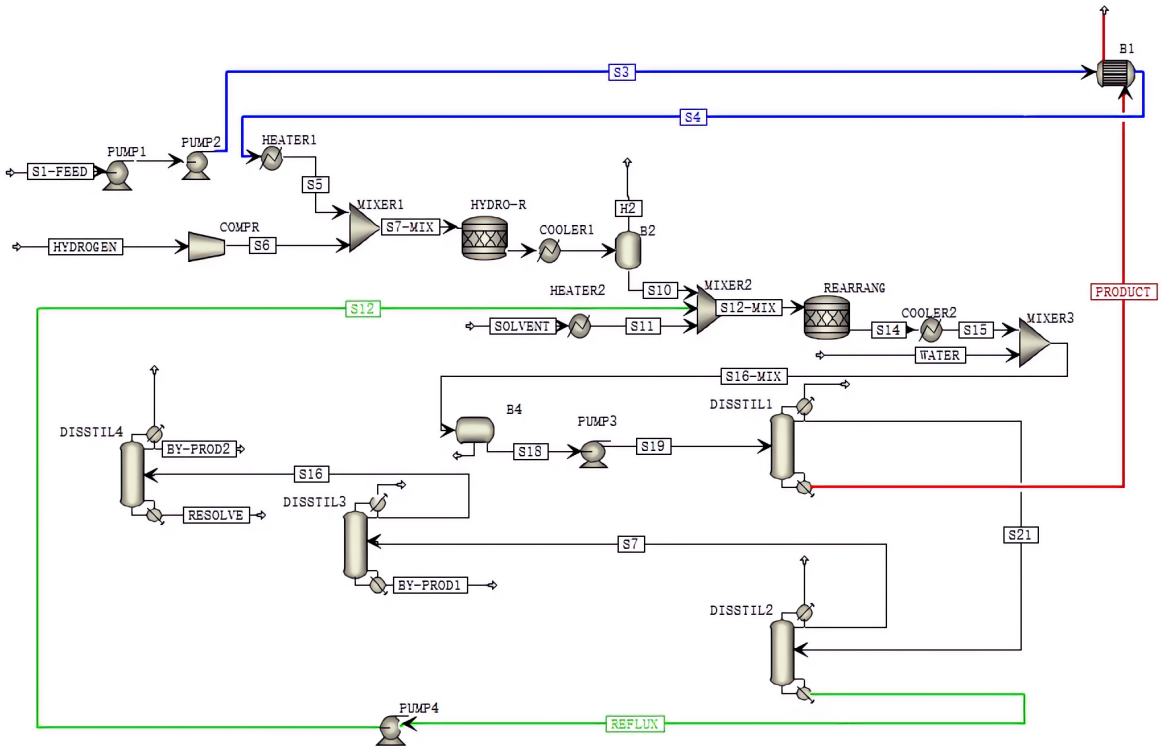

Figure 8. Technological process for producing aviation fuel from sesquiterpenes.

2.3.2. Process Concept and Design

The full-process physical properties method uses the PENG-ROB method, which is based on the PENG-Robinson cubic equation of state, which calculates all thermodynamic properties except the molar volume of the liquid. It is suitable for non-polar or weakly polar mixtures, such as hydrocarbons and light gases (such as CO_2, H_2S and H_2). It is suitable for high temperature and high pressure ranges. It is often used in gas processing, oil refining and petrochemical applications, and is suitable for the process of producing aviation fuels from sesquiterpenoids.

Hydrogenation Section

Using α-longipinene as the raw material of a sesquiterpene compound, hydrogenated α-longifolene was obtained through hydrogenation reaction. The hydrogenation reaction conversion rate was 99.8%. The reaction was operated adiabatic in a 120 L hydrogenation reactor. The α- longipinene material is transported at a constant flow rate by a feed pump. Before entering the hydrogenation reactor, it is heated to 320 °C by a heater. Hydrogen is pressurized into the top of the reactor through a compressor and reacts under the action of a catalyst. The pressure of the reactor is controlled by adjusting the opening of the valve on the feed hydrogen pipe. The reaction products are discharged from the bottom to the hydrogenation separation tank. The gas phase at the top of the tank is small and discharged directly, and the liquid-phase reaction products at the bottom enter the next section. The design of this section refers to the direct hydrogenation reaction of farnesene at a temperature of 320 °C and a pressure of 40 bar [1] and the pyrolysis gasoline hydrogenation process technology. The hydrogenation reaction equation of α-longifolene is as follows:

$$C_{15}H_{24} + H_2 \rightarrow C_{15}H_{26} \quad (4)$$

The hydrogenation reactor adopts the RStoic reactor model in Aspen. The RStoic model is suitable for chemical reactions with known reaction degrees or conversion rates. In the literature test results, the hydrogenation reaction is almost completely carried out, so the conversion rate of α- longipinene is set to 99.8%. The hydrogenation product in the reactor after this reaction is in the gaseous phase, which needs to be transformed into the liquid phase through subsequent cooling operations and then enters the rearrangement reactor.

Rearrangement Section

The hydrogenation product of the rearrangement section and the solvent 1,2-dichloroethane are mixed and then entered the rearrangement reactor. The rearrangement reaction takes place under the catalytic conditions of

40 °C, 1 bar and Lewis acid to obtain three alkyl diamondanes with a total yield of 65.1%. They are trimethyl-ethyl-adamantane($C_{10}H_{16}$), pentamethyl-adamantane($C_{10}H_{16}$), and ethyl-propyl-adamantane($C_{10}H_{16}$). They are named TEAM, PMAM, and EPAM according to their English names. At the same time, some by-products are produced. The main components of the by-products are alkylcyclohexane and alkylnaphthalene, which can be recycled for the production of other chemicals. The yields of the main product and by-products are as follows in Table 3. The mixed product is alkali washed with a mixed solution of sodium hydroxide and sodium chloride to remove acidic impurities. After the liquid is allowed to stand and layered, the upper organic liquid and the lower aqueous phase are separated, and the organic liquid enters the next rectification section for separation operation.

Table 3. Rearrangement reaction equation.

	Reaction Equation	Conversion Rate
Main reaction	$C_{15}H_{26} \rightarrow$ TEAM ($C_{15}H_{26}$)	30.7%
	$C_{15}H_{26} \rightarrow$ PMAM ($C_{15}H_{26}$)	11.8%
	$C_{15}H_{26} \rightarrow$ EPAM ($C_{15}H_{26}$)	22.6%
Side reactions	$C_{15}H_{26} \rightarrow C_7H_{14} + C_8H_{12}$	2.5%
	$C_{15}H_{26} \rightarrow C_8H_{16} + C_7H_{10}$	2.5%
	$C_{15}H_{26} \rightarrow C_9H_{18} + C_6H_8$	2.5%
	$C_{15}H_{26} \rightarrow C_{10}H_{20} + C_5H_6$	2.5%
	$C_{15}H_{26} \rightarrow C_{11}H_{20} + C_4H_6$	10.5%

Hydrogenated α-longipinene $C_{15}H_{26}$ was in the gaseous phase before entering the rearrangement reactor, with a temperature of 320℃. Before entering the reactor, the temperature was 320℃, and a condenser COOLER1 was set to reduce the temperature to 40℃. The solvent 1,2-dichloroethane is heated from room temperature to 40 ° C through a heater HEATER2. The first batch of solvent fed needs to be heated up by heater HEATER2. The heater HEATER2 can be canceled after there is reflux hot stream raw material. The temperature of the reflux raw material stream becomes 53℃ after being mixed with solvent and other materials, which is higher than the rearrangement reactor. The reaction temperature, so it is necessary to set up a condenser COOLER2 in front of the rearrangement reactor to reduce the temperature to reach the reaction temperature. The hydrogenation products enter the rearrangement reactor, which still adopts the RStoic model. There is no module for direct solid-liquid separation in Aspen Plus, so there is no Lewis acid catalyst in the rearrangement reactor. Assuming that the catalyst required for the reaction is packed at the bottom, the solid catalyst and the liquid phase product are separated in layers after the reaction. The rearrangement reaction conditions are temperature 40℃ and atmospheric pressure 1 bar. The mixed material finally flowing out of the reactor includes unreacted hydrogenated α- longipinene $C_{15}H_{24}$, alkyldiamondanes, by-products, and solvent, and the mixture flow enters the alkali washing stage.

The setting of flash tank B4 has two functions: one is to discharge trace excess hydrogen in the system; the other is to alkali wash the rearrangement product. After the liquid is left and layered, the upper organic liquid and the lower aqueous phase are separated. The flash tank temperature is set to normal temperature of 25 °C and atmospheric pressure of 1 bar. 10% NaOH solution, sodium chloride NaCl solution and the cooled rearrangement product are mixed and entered into the flash tank module; a trace amount of excess hydrogen in the hydrogenation reaction is discharged from the top of the tank; after alkali washing and layering, the upper organic phase stream S17 enters the next stage. At the next stage, the lower aqueous phase is discharged from stream S14. The aqueous phase stream contains acidic catalysts and cannot be reused.

Rectification Section

The mixed stream enters the rectification and rectification column DISSTIL1 through a flow pump. After the reboiler is heated, the alkyl diamondane product with a mass fraction of more than 99% is distilled from the bottom of the rectification column DISSTIL1. The condenser at the top of the rectification column DISSTIL1 is partially condensed. A small amount of uncondensed organic light gas is collected into the storage tank. The condensed liquid phase includes hydrogenated α-long-leaf pinene that has not undergone rearrangement reaction, by-products, and solvent. The condensed stream enters the next rectification column for separation. The temperature of the product stream at the bottom of the tower is relatively high, and a heat exchanger is used to exchange heat with the α-longifolene feed stream, reducing heating requirements.

The condensed liquid phase enters DISSTIL2, and the hydrogenated α- longipinene that has not undergone rearrangement reaction distillates from the bottom of the rectification column. A small amount of uncondensed light gas, condensed solvent and by-products distillates from the top of the column. The hydrogenated α-

longipinene that has not undergone rearrangement reaction is refluxed into the rearrangement reactor to continue the reaction. The solvent and by-product streams enter the next rectification column for separation.

Since the boiling points of 1,2-dichloroethane and C_7H_{14}, C_7H_{10} and C_6H_8 are similar, two towers are set up to separate 1,2-dichloroethane and by-products. C7-C10 by-products are distilled from the bottom of the DISSTIL3 column. The condensed liquid phase at the top of the column enters DISSTIL4, where 1,2-dichloroethane that can be used for reflux is distilled off, and the overhead condenser distills off C4-C7 by-products.

The bottom of the rectification column DISSTIL1 discharges the rearrangement product, alkyl diamondane aviation fuel product, and the top of the column discharges unreacted hydrogenated α- longipinene, by-product and solvent 1,2-dichloroethane. The top of the column is set as a semi-condenser, and a small amount of gaseous substances is discharged from the top of the column; The top of the rectification column DISSTIL2 discharges a mixture of solvent 1,2-dichloroethane and by-products, and the bottom of the column containing a small amount of gas phase discharges unreacted hydrogenated α-longipinene for reflux, which reduces raw material waste and increases yield. The top mixture flows into the next rectification column DISSTIL3. Since the boiling points of solvent 1,2-dichloroethane and by-products are similar, the rectification column DISSTIL3 cannot completely separate 1,2-dichloroethane and by-products. The by-product C_7H_{14} and by-products with a molecular weight higher than C_7H_{14} are distilled off at the bottom of DISSTIL3 and enter the storage tank; the top stream S10 distills the solvent, C_7H_{14} and by-products with a molecular weight lower than C_7H_{14} and enter the next rectification column DISSTIL4. By-products and a small amount of solvent with a molecular weight lower than C_7H_{14} are distilled off at the top of DISSTIL4, and the solvent 1,2-dichloroethane with a mass fraction of 99.8% is distilled off at the bottom of the column for reflux and reuse.

2.3.3. Mass and Energy Balances

Based on the above simulations, the of materials and energy are obtained in Table 4.

Table 4. Energy requirements of each module.

Module	Public Works	Value	Unit
PUMP1	Electricity	0.0083	kW
PUMP2	Electricity	0.046	kW
PUMP3	Electricity	<0.0001	kW
PUMP4	Electricity	0.0014	kW
COMPR	Electricity	0.46	kW
HEATER1	Electricity	1.56	kW
HEATER2	170 °C Steam	0.021	kg/hr
COOLER1	Condensed water	119.5	kg/hr
COOLER2	Condensed water	11.1	kg/hr
DISSTIL1 Condenser	Condensed water	199.9	kg/hr
DISSTIL1 Reboiler	226 °C Steam	11.5	kg/hr
DISSTIL2 Condenser	Condensed water	120.3	kg/hr
DISSTIL2 Reboiler	170 °C Steam	7.65	kg/hr
DISSTIL3 Condenser	Condensed water	79.2	kg/hr
DISSTIL3 Reboiler	170 °C Steam	1.2	kg/hr
DISSTIL4 Condenser	Condensed water	33.5	kg/hr
DISSTIL4 Reboiler	170 °C Steam	0.6	kg/hr

3. EIA of the Sweet Sorghum Transformation to Bio-Aviation Fuel

3.1. The Fossil Fuel Aviation Fuel as Reference Case

3.1.1. Production and Transportation

According to Cai's [13] project survey and the annual report provided by the U.S. Energy Information Administration, 79.77% of the refined crude oil supply is obtained through direct mining, 12.92% is obtained through cracking chemical reactions and transformation of oil shale; and 7.3% is obtained through oil sands refining. Among them, mining oil sands to obtain synthetic crude oil includes the following four technologies: open-pit mining of oil sands synthetic crude oil, open-pit mining of asphalt, on-site production of synthetic crude oil, and on-site production of asphalt, accounting for 41.7%, 5.3%, 6.0%, and 47.1% respectively.

According to the investigation and research of Sun et al.[14], the refining efficiency of traditional aviation fuels is 91.1%. The main energy use of refineries is distributed among refining distillate gas, natural gas and refining catalyst coke. Pollutant emissions from the combustion of these energy sources account for 91% to 100%

of total pollution emissions. The use of other fuels, such as coal, distillate oils and residual fuel oils, accounts for only a small portion of total emissions.

The crude oil transportation is a major contributor to the EIA assessment. Take crude oil transportation to China as an example, 90% of imported crude oil needs to be transported domestically by ocean-going tankers. In 2022, more than 75% of China's imported crude oil will come from outside Asia, with imports from the Middle East accounting for 53%. Shipping mileage will exceed 5800 nautical miles, and transportation will take more than 20 days; Africa and the Americas import volume will both be about 10%, the mileage is close to 10,000 nautical miles, and transportation will take more than 35 days. The remaining 10% of imported crude oil is imported through pipelines.

90% of imported crude oil is transported to China by ocean cruise ships. Ships transport crude oil from non-Asian regions accounts for 77%. Non-Asian regions are mainly the Middle East, America, Africa, Russia, etc., and crude oil from the Asian region accounts for 23%. The Asian region is mainly Southeast Asia and other places. After years of exploration, my country's crude oil shipping routes have been basically stable, forming the following major shipping routes: (1) Middle East routes (2) African routes, including West Africa, North Africa, East Africa and South Africa routes (3) Latin American routes, including Panama branch and transatlantic routes (4) North America routes (5) Nordic routes (6) Russian routes (7) Southeast Asia routes. The Middle East route mainly refers to starting from the Persian Gulf, passing through the Strait of Hormuz, entering the Indian Ocean through the Arabian Sea, then reaching the South China Sea of China through the Strait of Malacca, and finally reaching the coast of China. The North African route starts from North Africa, passes through the Suez Canal, enters the Red Sea, the Gulf of Aden, and the Arabian Sea, then passes through the Indian Ocean, the Strait of Malacca, enters the South China Sea of China, and reaches China's coastal ports. One Latin American route refers to the route to the coast of China via the Cape of Good Hope, the Indian Ocean, and the Strait of Malacca. This route is suitable for shipping by super-large cruise ships; the other is the route to the coast of China via the Panama Canal and the Pacific Ocean. Shipping of North American (mainly the United States) crude oil to China will travel through the Pacific Ocean to the coast of China. The Nordic route is mainly for the transportation of Norway crude oil to China. It usually follows the Atlantic Ocean on the west coast of Europe southward. The lighter ones can enter the Strait of Gibraltar, enter the Mediterranean Sea, pass through the Suez Canal, and go directly to the Red Sea, along the Arabian Sea—Indian Ocean—Malacca—China South China Sea route. The shipping route from Russia to China cannot transport directly from the Far East to China. Instead, it must depart from ports in Europe to reach China via the Suez Canal or detour through the Cape of Good Hope in southern Africa. This distance is used as the distance for transporting crude oil from the Middle East. Crude oil transportation in the Middle East accounts for more than 50% and is calculated based on 50%. The shipping distance from Suez to Shanghai, China is 13,126 km. This distance is used as the distance for transporting crude oil from Africa, which accounts for 30% of crude oil transportation; Taking the distance from Los Angeles in the United States to Songhu Port in Shanghai in China of 11,560 km as the distance of the American route, calculated at 7%; the distance from the Suez Canal for the Russian route is calculated at 13,126 km, and Russia's ocean transportation volume accounts for 6%; taking the distance from Malaysia to Sinochem Quanzhou Petrochemical Terminal of 3050 km as the crude oil transportation distance in the Asian region, and the Asian regional transportation volume accounts for 7% of the ship transportation volume. 10% of imported crude oil is transported through pipelines [15], which include the China-Russia Channel with a total length of ~1000 km, the China-Myanmar Channel with a domestic total length of 1631 km, and the China-Kazakhstan crude oil pipeline with a total length of 2798 km.

3.1.2. Conventional Jet-Fuel Distribution

The present study investigated the distance from some large refining plants to large airports which is shown in Table 5. The main transportation method for aviation kerosene at domestic airports is railways. Most of the railways are close to refineries, have low transportation costs and adjustable transportation volume. Other transportation methods are road transportation, pipeline transportation and cruise transportation: road transportation is generally used for short-distance transportation of small and medium-sized airports, pipeline transportation is mostly used for short-distance transportation of domestic medium and large airports, and oil tanker transportation mainly ensures the oil consumption of domestic coastal airports. The following are the collected distances from some domestic refining plants with a capacity of more than 10 million tons to the airport:

Table 5. Distance from some domestic refining and chemical enterprises to the airport and methods of jet fuel transportation.

Refining and Chemical Enterprises	Airport	Aviation Fuel Transportation Method	Distance
Zhejiang petrochemical	Hangzhou Xiaoshan International Airport	Pipeline	210 km
Sinopec Tianjin	Tianjin Binhai International Airport	Pipeline	41 km
Sinopec Qingdao	Qingdao jiaodong International Airport	Pipeline	53 km
Sinopec Yunnan	Kunming changshui International Airport	Pipeline	57 km
PetroChina Lanzhou petrochemical	Lanzhou zhongchuan International Airport	Pipeline	65 km
Sinopec Luoyang branch	Zhengzhou Xinzheng International Airport	Pipeline	178 km
Maoming petrochemical	Guangzhou Baiyun International Airport	Pipeline	362 km
Maoming petrochemical	Chengdu Tianfu International Airport	Pipeline	1540 km
Maoming petrochemical	Chengdu Shuangliu International Airport	Pipeline	1595 km
Maoming petrochemical	Kunming changshui International Airport	Pipeline	1140 km
Liaoyang petrochemical	Shenyang Taoxian International Airport	Highway	93 km

Medium and large airports mainly use pipeline and railway transportation, calculated based on 50% of pipeline transportation and railway transportation volume. According to the above survey, the average distance of pipeline transportation is 100 km, and the average distance of railway transportation is 1158 km.

With respect to the distribution path for bio-aviation fuels in China, as from 19 September 2024, Sinopec Zhenhai Refining and Chemical (Zhenhai, China) started to provide sustainable aviation fuel for 12 flights of Air China, China Eastern Airlines and China Southern Airlines at Beijing Daxing, Chengdu Shuangliu, Zhengzhou Xinzheng and Ningbo Lishe Airports. The following is the distance from Zhenhai Refining and Chemical to these airports and the method of jet fuel transportation. These data are summarized in Table 6 below.

Table 6. Distance from Zhenhai Refining and Chemical Co., Ltd. to the airport and sustainable aviation fuel transportation methods.

Refining and Chemical Enterprises	Airport	Aviation Fuel Transportation Method	Distance
Zhenhai refining	Beijing Daxing International Airport	Railway	1345 km
Zhenhai refining	Zhengzhou Xinzheng International Airport	Railway	1025 km
Zhenhai refining	Chengdu Shuangliu International Airport	Railway	2035 km
Zhenhai refining	Ningbo lishe International Airport	Pipeline	200 km

Based on the above investigation, it is determined that taking Zhenhai Refining and Chemical as an example for transporting sustainable aviation fuel, the railway transportation of aviation fuel accounts for 75% of the transportation volume, with an average mileage of 1467 km, the pipeline transportation volume accounts for 25%, and the transportation mileage is 200 km.

3.2. The EIA of the Sorghum Agro and Sesquiterpene Process

The overall mass and energy balances are presented in Figure 9 to encompass the sorghum agro-logics, the straw transportation and its pretreatment. Processes involve fermentation, bio-aviation fuel upgrading, its storage and further “for flight” application. The overall process route from sweet sorghum to bio-aviation fuel is systematically illustrated in Figure 9.

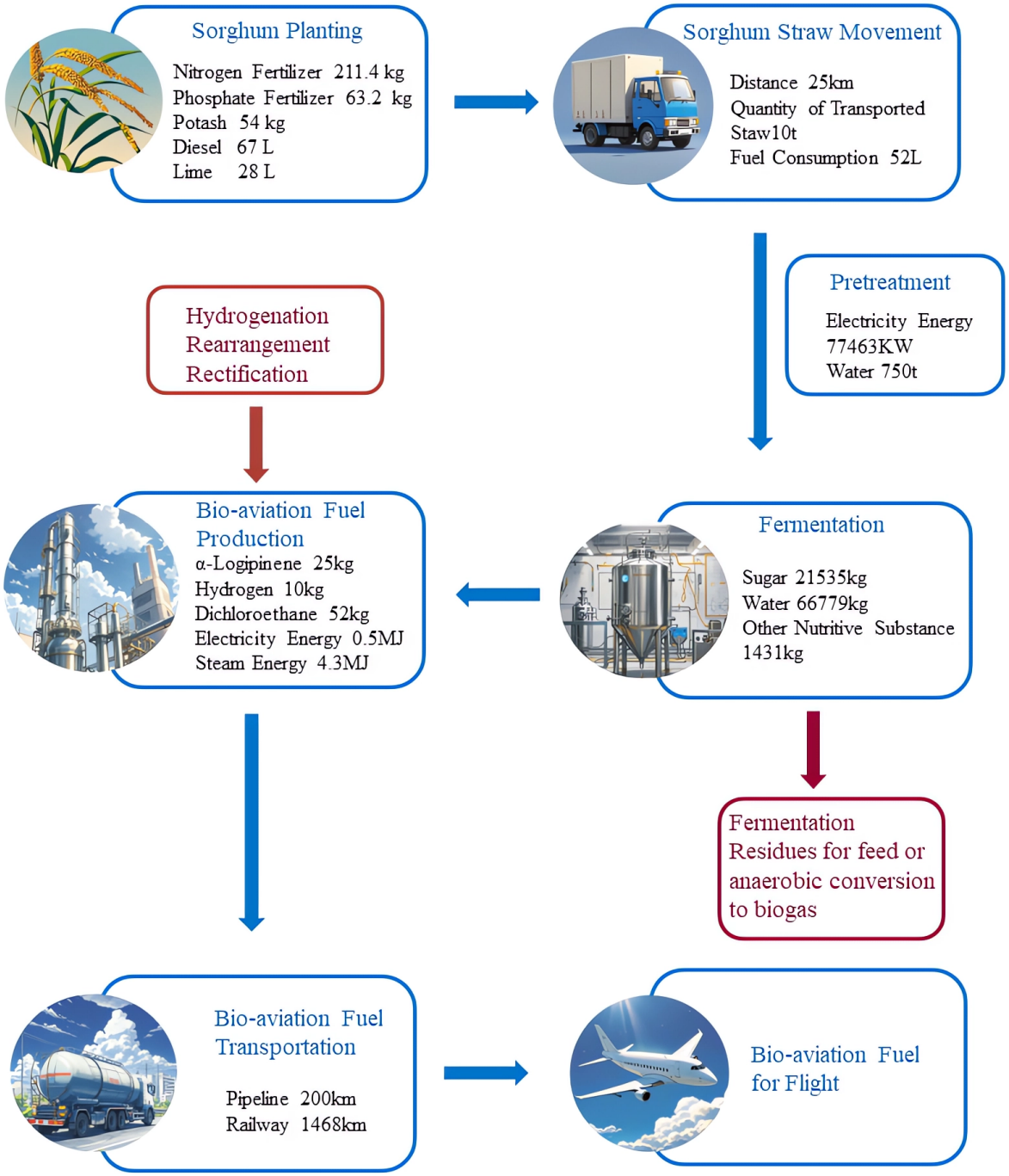

Figure 9. Process from sweet sorghum to bio-aviation fuel.

3.2.1. Carbon Footprint and Pollutant Emissions

According to the established process, the life cycle inventory results are obtained, that is, the emissions of various pollutants, and carbon dioxide emissions account for more than 99%. The following Figure10 is the carbon footprint of the process and the emission map of pollutants other than carbon dioxide.

Carbon dioxide emissions are caused by the production process or use of substances, and the production processes of diesel, hot steam, and some raw materials contribute significantly. Diesel fuel has high carbon emissions. First, due to the large amount of sorghum straw transported and the large number of round-trip transportation, which consumes more diesel. Second, after diesel is burned, the exhaust gas releases a large amount of carbon dioxide and other pollutants. The high carbon dioxide emissions of steam are due to the fact that steam is heated by natural gas boilers. The main product of the heating process is CO_2. At the same time, a small amount of H_2S and nitrogen in natural gas will burn to produce sulfur oxides and nitrogen oxides. Another major contribution to carbon emissions is caused by the raw material production process. The main reason is that the production process of hydrochloric acid, phosphate ore, potassium hydroxide and other substances consumes more

energy. In the process of fermentation and production of sesquiterpenes, nutrients such as potassium dihydrogen phosphate and ammonium sulfate are needed. Among them, potassium dihydrogen phosphate is prepared from phosphoric acid, urea and potassium hydroxide in a multi-step manner. For every 1 ton of potassium dihydrogen phosphate produced, 0.79 tons of phosphoric acid is consumed. The demand for phosphoric acid is large, while phosphoric acid is prepared by using phosphate ore and hydrochloric acid through a purification wet process. Among them, the phosphate ore is a medium-grade phosphate ore with a P_2O_5 content of 30%, and the mass fraction of hydrochloric acid is 39.2%, that is, for every ton of phosphoric acid produced, 3.33 tons of phosphate ore and 1.21 tons of hydrochloric acid are consumed. These two upstream processes lead to large consumption of hydrochloric acid and phosphate rock and high carbon dioxide emissions, that is, the carbon emissions of raw materials are mainly contributed by potassium dihydrogen phosphate and ammonium sulfate in the fermentation production stage of sesquiterpenes. Electricity, as a less used energy source, contributes little to carbon emissions.

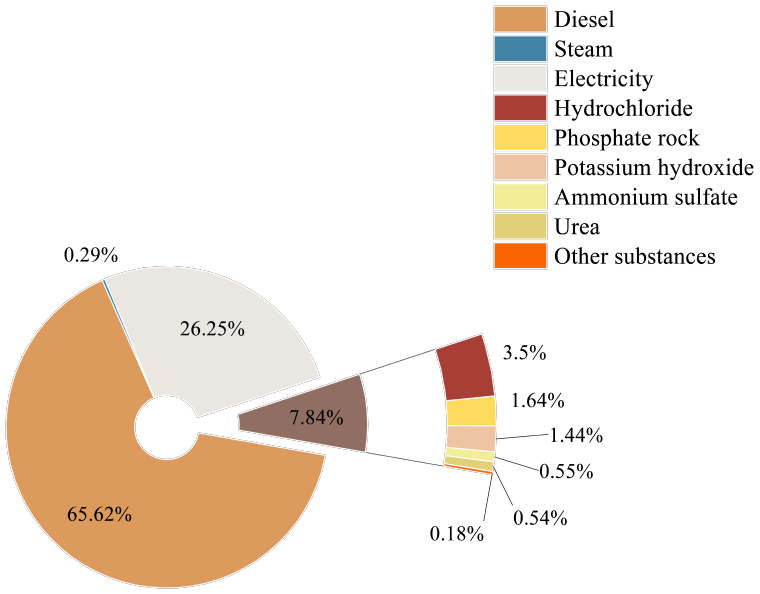

Figure 10. Main pollutants emissions of sustainable aviation fuel.

In addition to carbon dioxide, the proportion of other pollutants emissions is shown in Figure11. It can be seen that methane emissions are more than other polluting gases. First, because there are more diesel, natural gas, coal and other substances used in the system, their mining and production processes will emit more methane. Second, sweet sorghum During the planting process, methanogenic bacteria can convert organic matter into methane in an anaerobic environment. Third, fermentation waste liquid will be generated during the fermentation process. During waste liquid treatment, the anaerobic environment will also lead to the production of methane. After diesel is burned, the exhaust gas not only releases a large amount of carbon dioxide, but also releases $PM_{2.5}$ and NO_x, and diesel will produce CO and soot particles when it is not completely burned. When natural gas boilers are heated to produce steam, small amounts of nitrogen and H_2S will burn to produce NO_x and SO_x. Sorghum is a low-sulfur biomass, with a sulfur content ranging from approximately 0.05% to 0.3%.

Due to the large consumption of diesel, six processes have been set up to examine the sensitivity of carbon dioxide emissions using GWP indicators. These six scenarios are listed in Table 7 below.

Table 7. Changes in different scenarios.

Scenarios	Uncertain Factors	Change Amount
1	Proportion of biodiesel in transport trucks	+20%
2	Proportion of biodiesel in transport trucks	+40%
3	Transportation distance	+20%
4	Transportation distance	-20%
5	Single transportation volume of straw	+20%
6	Single transportation volume of straw	-20%

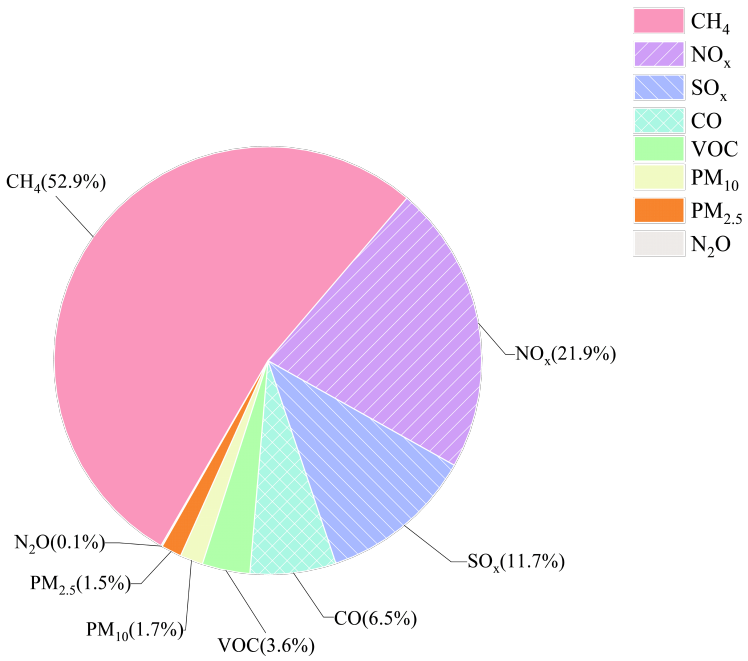

Figure 11. Emissions of pollutants other than CO_2.

As shown in Figure 12, the sensitivity analysis results of different scenarios clearly reflect the impact of key variables on the target index, which provides a basis for the robustness verification of the model. For every 20% increase in the amount of biodiesel, the contribution to GWP decreases linearly by 7.09%; when the transportation distance changes within the range of 20%, the GWP changes within the range of ±10.3%, indicating that compared with the increase in biodiesel, GWP is more sensitive to the transportation distance; the increase and decrease of a single transportation volume of straw will lead to irregular changes in the number of transportation times; within the range of 20% transportation volume, GWP is more sensitive to the reduction of straw transportation volume than the increase of single transportation volume.

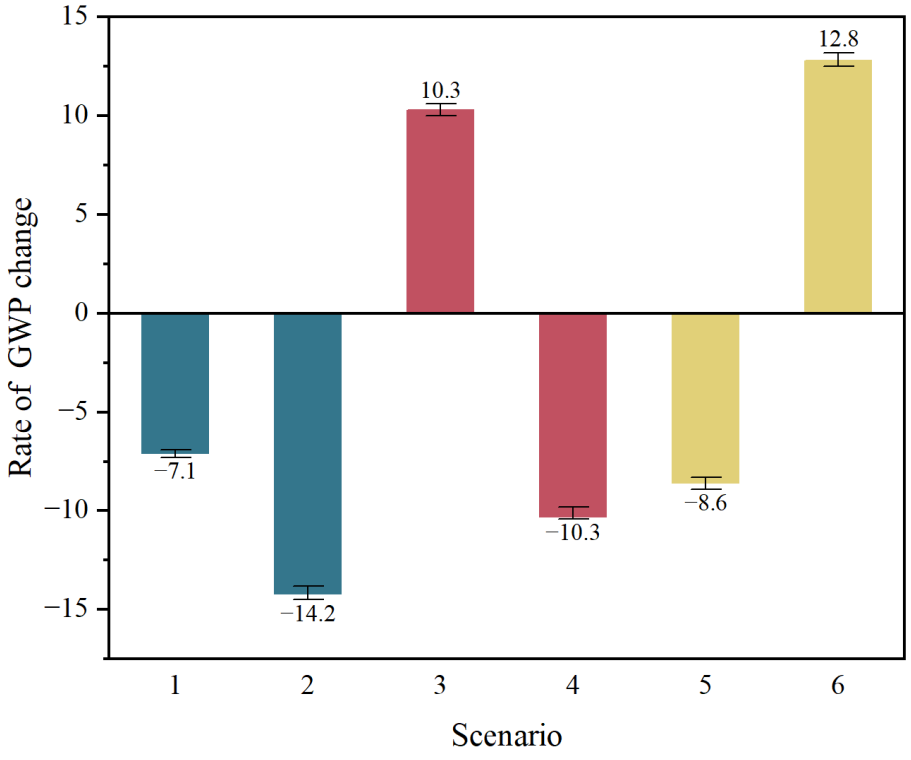

Figure 12. Sensitivity analysis results of different scenarios.

3.2.2. Comparation of Environmental Impacts at Various Stages

Recipe 2016 has a total of 17 impact indicators. This study selected 8 midpoint environmental impact indicators and 3 endpoint environmental impact indicators. The following is a brief introduction to the selected indicators:

(1) GWP: The characteristic factors of climate change are expressed in terms of global warming potential. Based on carbon dioxide, 1 unit of carbon dioxide has the ability to warm the earth, and other gases are expressed in terms of their relative values. The global warming potential value will change over time. The method uses the 2013 report of the Intergovernmental Panel on Climate Change (IPCC) and uses 120 years of global warming potential as the control standard, in units of kg CO_2 to air equivalent
(2) PMFP: The characteristic factor of fine particulate matter is expressed by the inhalation amount of $PM_{2.5}$, and the unit is kg $PM_{2.5}$ to air equivalent
(3) HOFP: Human health ozone formation potential represents the extent to which ozone is harmful to human health (the frequency and severity of human respiratory distress, such as asthma and chronic obstructive pulmonary disease), in units of kg NO_x to air equivalent
(4) EOFP: Ecosystem ozone formation potential represents the damage to terrestrial ecosystems caused by ozone emissions, in units of kg NO_x to air equivalent
(5) TAP: The criterion for measuring land acidification is the acidification potential, using the world average lethal dose of SO_2 as the characteristic value, that is, the difference between the actual life expectancy and the ideal life expectancy per kilogram of SO_2 intake, in units of kg SO_2 to air equivalent
(6) FEP: Freshwater eutrophication potential represents the degree of eutrophication of fresh water, agricultural soil and seawater by phosphorus and phosphate
(7) MEP: Marine eutrophication potential represents the extent of dissolved inorganic nitrogen (DIN). released into fresh water (rivers), soil and coastal waters in kg N-eq to marine water equivalent
(8) FFP: The fossil fuel potential of fossil resource x is defined as the ratio of the energy content of fossil resource x to the energy content of crude oil, in units of kg P to freshwater equivalent
(9) HH: Damage to human health (HH) measures the extent of human health loss caused by the research object. The unit year refers to the equivalent year of health loss (based on Disability-Adjusted Life Year, DALY)
(10) ED: Destroy ecosystem quality (ED) evaluates the degree of damage to ecosystem structure and function induced by the research object. The unit species/yr denotes the annual species loss
(11) RA: Damage to resource availability (RA) characterizes the impact of the research object on the sustainable utilization of natural resources. The unit Dollar represents the monetized value of resource consumption.

The above environmental impact indicators are selected because the sesqui-based bio-aviation fuels will inevitably emit CO_2, SO_x, $PM_{2.5}$, and NO_x during the production process. On the one hand, the increase in the concentration of these greenhouse gases will increase the radiation forcing ability. Radiative forcing capacity, a core term in the field of climate science, refers to the ability of greenhouse gases and other factors to perturb the balance of the atmospheric energy budget. The higher its value, the stronger its driving effect on global warming. On the other hand, rising temperatures will eventually cause damage to human health and ecosystems. The upstream path of the production process will also involve the extraction of crude oil and natural gas, resulting in the reduction of natural resources. During the S1 sweet sorghum planting stage, nitrogen and phosphorus will be released into the soil during the fertilization process, resulting in a certain degree of freshwater eutrophication and seawater eutrophication. Freshwater eutrophication occurs due to the release of nutrients into soil or freshwater bodies and the subsequent increase in nutrient levels (i.e., phosphorus and nitrogen). There are many environmental impacts associated with freshwater eutrophication. They follow a series of ecological impacts that are offset by increasing nutrient discharges into freshwater, thereby increasing nutrient uptake by autotrophic organisms such as cyanobacteria and algae, and heterotrophic species such as fish and invertebrates, which ultimately leads to relative loss of species. In this research work, the impact of nitrogen and phosphorus emissions on freshwater is based on the transfer of nitrogen and phosphorus from soil to freshwater bodies, their residence time in freshwater systems, and what may disappear as nitrogen and phosphorus concentrations in freshwater increase. Marine eutrophication occurs due to the run-off and leaching of plant nutrients from the soil, and the release of these nutrients into rivers or ocean systems, and the subsequent increase in nutrient levels, namely phosphorus and nitrogen. In this research work, the impact on seawater was based on the transfer of dissolved inorganic nitrogen (DIN) from soil and freshwater bodies. The causal chain of dissolved inorganic nitrogen (DIN) emissions, including diffuse sources (soil runoff and leachate) and point sources (direct emissions) to rivers and coastal waters, causes a loss of marine species richness.

In order to determine the impact of the bio-aviation fuel process on various aspects of the environment in this study, Tables 8 and 9 below present the indicators used for calculation and analysis.

Table 8. Recipe method endpoint impact indicators.

Endpoint Impact Indicators	Abbreviation	Units
Damage to human health	HH	year
Destroy ecosystem quality	ED	species/yr
Damage to resource availability	RA	Dollar

Table 9. Recipe method midpoint impact indicator.

Mid-Point Impact Indicator	Abbreviation	Units	Life Cycle Inventory Substances
Global warming potential	GWP	kg CO_2 to air	CO_2, CH_4, N_2O…
Particulate formation potential	PMFP	kg $PM_{2.5}$ to air	$PM_{2.5}$
Human health ozone formation potential	HOFP	kg NO_x to air	Nox, NMVOC
Ecosystem ozone formation potential	EOFP	kg NO_x to air	Nox, NMVOC
Land acidification potential	TAP	kg SO_2 to air	SO_2, NO_x…
Freshwater eutrophication potential	FEP	in kg P to freshwater	P, P_4^{3-}…
Marine eutrophication potential	MEP	In kg N-eq to marine water	N, NH_4^+, NO_2…
Fossil fuel potential	FFP	kg oil	Crude oil, Natural gas, Hard coal

In this study, the production process of the bio-aviation fuel production stage is divided into six stages, and the six stages are S1 sweet sorghum planting stage, S2 sweet sorghum straw transportation stage, S3 straw pretreatment stage, S4 straw sugar fermentation stage to produce sesquiterpenes, S5 sesquiterpenes refining into aviation fuel stage, and S6 bio-aviation fuel transportation stage. As shown in Figure 13, the mid-point environmental impact indicators for each stage of the process exhibit distinct variation trends, which can directly reflect the environmental load distribution characteristics of the whole production chain.

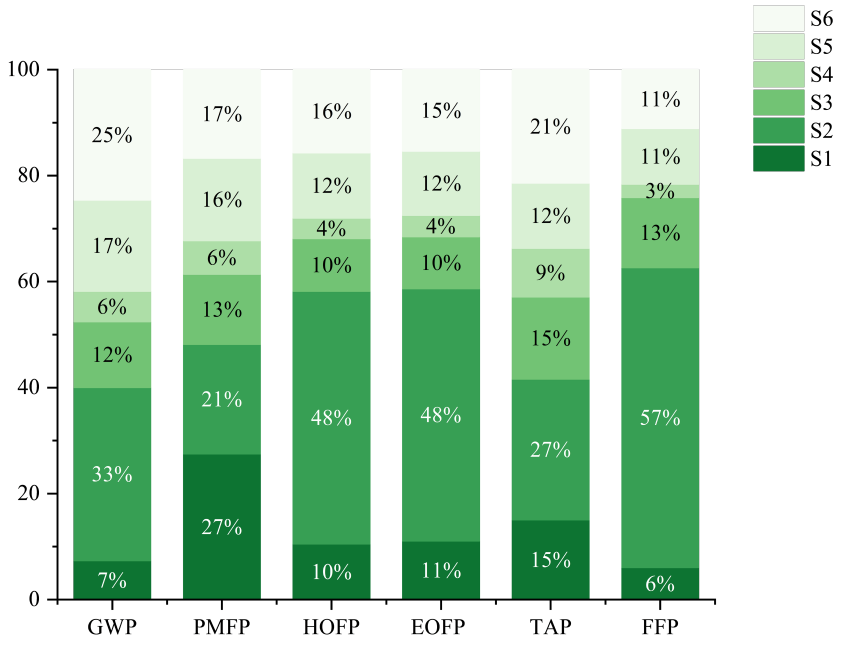

Figure 13. Midpoint environmental impact indicators for each stage.

Only the S1 sweet sorghum planting stage has an impact on MEP and FEP environmental indicators. Because nitrogen and phosphate fertilizers are released into the soil during the planting stage, 10% of phosphorus and 13% of nitrogen in the soil are transferred to surface water. The contribution of the remaining indicators is mainly the harvest, storage and transportation stage of S2 sweet sorghum straw, where a large amount of diesel is burned during the transportation process, resulting in more CO_2, N_2O, $PM_{2.5}$, SO_2, NO_x, and VOC emissions. Compared with other stages, the proportion of environmental impact indicators in stage S2 is significantly larger, with an average proportion of 47%. Including the transportation process of aviation fuel, transportation throughout the entire process accounts for 64.5% of the environmental impact. Agricultural machinery used in the S1 sweet sorghum planting stage, such as seeders, transplanters, etc., consume diesel, increasing the emission of various

pollutants; The stage S3 of sweet sorghum straw pretreatment accounts for an average of 11.17% of the environmental impact indicators, which mainly uses crushers (straw juicing) and evaporators (glucose concentration). These machines consume a certain amount of electricity, and the upstream of electricity is mainly coal and natural gas combustion to generate electricity. The stage S4 of sesquiterpenes fermentation has less contribution to various indicators. This is due to mild fermentation conditions, short operating time and low stirring speed of the fermentation tank agitator, and low-power electrical appliances. As a result, both the total power consumption and the amount of steam used for disinfection and sterilization of the fermentation tank are low. The upstream natural gas and coal combustion are reduced, resulting in lower upstream pollution emissions and energy consumption. The proportion of the environmental impact indicators in stage S5 of aviation fuel production is 13.33% on average, and the distillation column is the main energy-consuming unit in this stage. The upstream path for consuming steam and steam heat energy during the operation process is mainly the combustion of natural gas and coal and the continuous traceability upstream. The collection and transportation process of natural gas and coal mines will also emit CH_4, non-methane hydrocarbons, SO_2, NO_x, etc.

From the above analysis, the harvesting, storage and transportation stages of sweet sorghum straw contribute most of the pollution emissions and fuel consumption, and diesel emissions are inevitable. It is recommended to appropriately use biodiesel, which is made from renewable resources. (such as animal and vegetable oils, waste oils) are refined and have the characteristics of high cetane number, non-toxic, low-sulfur, degradable, and non-aromatic hydrocarbons. They produce fewer pollutants during combustion and have obvious effects on reducing the emission of hydrocarbons, carbon monoxide, sulfur oxides, particulate matter, etc. in diesel vehicle exhaust.

4. Comparation of Environmental Impact of Bio-Aviation Fuel and Petro-Aviation Fuels

In order to objectively analyze the environmental benefits of bio-aviation fuels using glucose as an intermediate, this study established a process based on traditional aviation fuels in China region for comparison, established a model for traditional aviation fuel production, and set the system boundaries from crude oil extraction to aviation fuel delivery.

The comparison results of midpoint and endpoint environmental impact indicators shown in Figures 14 and 15 provide a comprehensive basis for environmental performance evaluation. Except for the two indicators of MEP and FEP, traditional aviation fuel manufacturing far exceeds biological aviation fuel manufacturing for other environmental impact indicators. It shows that whether in terms of sulfur oxides, nitrogen oxides, carbon dioxide, particulate matter emissions, or fossil energy consumption, the process flow of traditional aviation fuels exceeds the process flow of biological aviation fuels; the comparison results of endpoint indicators can be seen that the hazards to human health, damage to ecosystem quality, and damage to resource availability of traditional aviation fuels is much higher than that of the biological aviation fuel manufacturing process. These environmental impact indicators show that bio-aviation fuels with sesquiterpenes as intermediates are clean aviation fuels with less pollution emissions and less energy consumption.

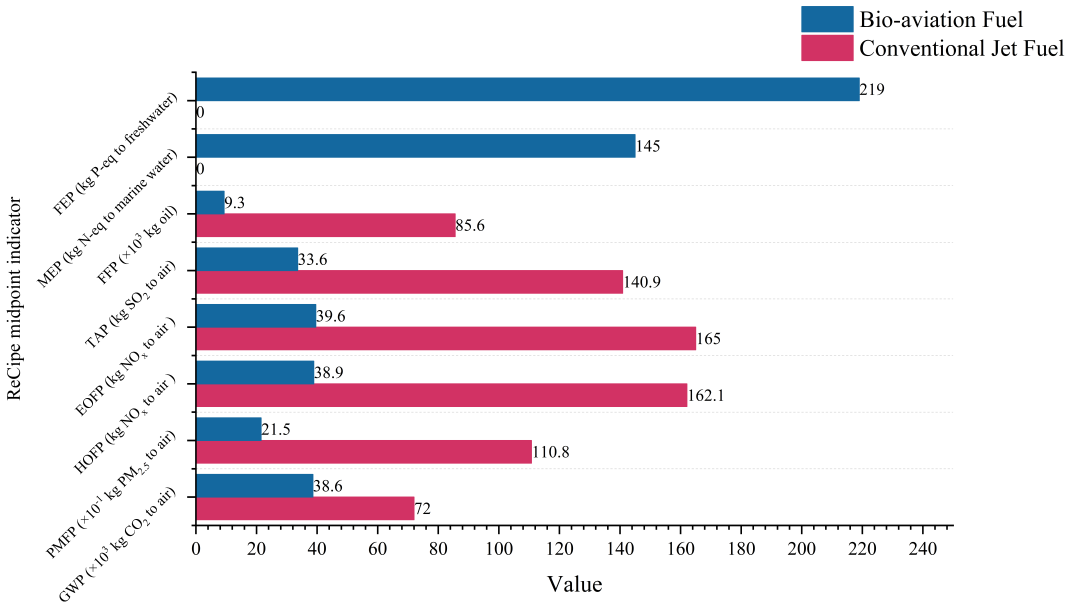

Figure 14. Comparison of midpoint environmental impact indicators.

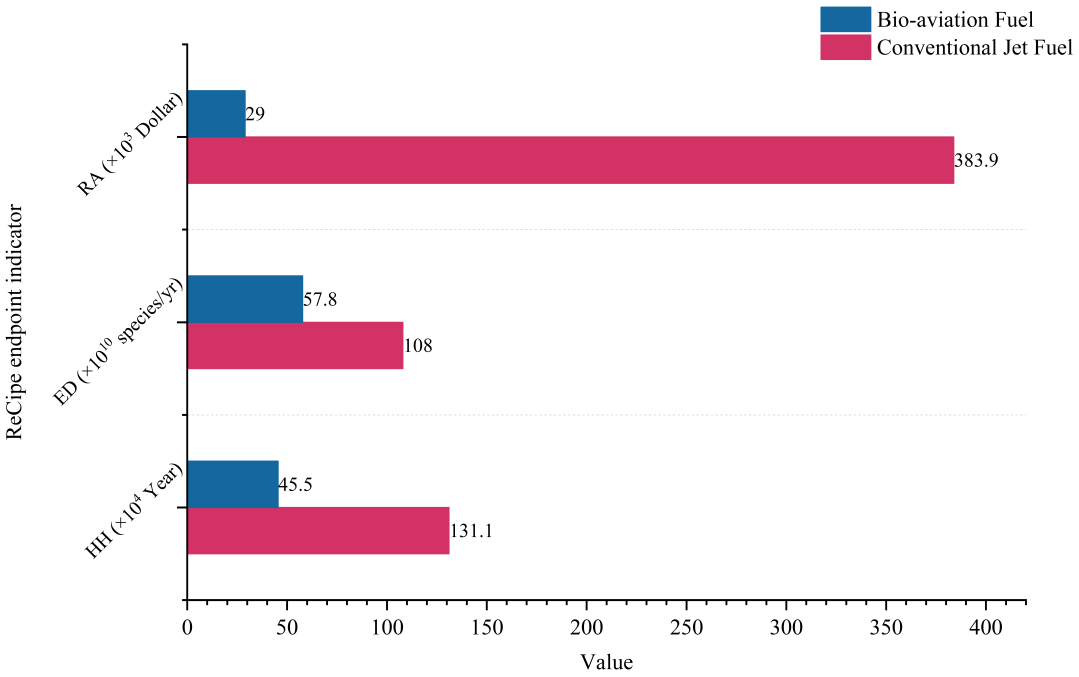

Figure 15. Comparison of endpoint environmental impact indicators.

5. Conclusions

This study presents a system that utilizes sweet sorghum straw as a carbon source, integrating processes such as cultivation, fermentation, transportation, and refining to produce bio-aviation fuel. Aspen Plus was employed to simulate the fermentation process and the process of refining sesquiterpenes into aviation fuel. Through conducting an Environmental Impact Assessment (EIA) of this system, it was found that the carbon footprint mainly comprises diesel and electricity, accounting for 65.62% and 26.25% respectively. Apart from CO_2, the other major pollutants are CH_4 and NO_x, accounting for 52.9% and 21.9% respectively. The mid-point environmental impact indicators of each stage of the system, determined that transportation accounted for 64.5%, straw pretreatment accounted for 11.17%, and the refining of sesquiterpenes into aviation fuel accounted for 13.33%. These stages are the key areas that require optimization and energy conservation. Finally, a comparison of the environmental impact indicators between this system and the traditional aviation fuel process using fossil fuel as a raw material was carried out. In terms of the performance of the end-point environmental impact indicators, the hazards to human health, ecosystem quality, and resource availability caused by traditional aviation fuel significantly exceed the bio-aviation fuel manufacturing process with sesquiterpenes as intermediates.

Overall, this research provides a valuable bio-aviation fuel production route and a prediction of the environmental impact of this solution.

Supplementary Materials: The following supporting information can be downloaded at: https://media.sciltp.com/articles/others/2512191616279531/SEE-25110127-Supplementary-Materials.pdf, Table S1: Sesquiterpene fermentation energy consumption (aspen simulation results); Table S2: Aspen-derived materials and Energy consumption during the conversion of sesquiterpenoids into aviation fuel.

Author Contributions: Y.J.: Conceptualization, Computation, Validation, Formal analysis, Investigation, Writing—original draft, Writing—review & editing; B.A.: Conceptualization, Computation, Investigation, Writing—original draft Writing—review & editing; J.Z.: Formal analysis, Investigation, Writing—review & editing; Y.K.: Formal analysis, Investigation, Writing—review & editing; H.Z.: Resources, Writing—original draft, Writing—review & editing, Supervision, Project administration; M.W.: Resources, Writing—original draft, Writing—review & editing, Supervision, Project administration. All authors have read and agreed to the published version of the manuscript.

Funding: The authors acknowledge the support of the National Key Research and Development Program of China (2021YFC2103700).

Data Availability Statement: Data can be obtained on request to the corresponding author.

Conflicts of Interest: The authors declare no conflict of interest.

Use of AI and AI-Assisted Technologies: During the preparation of this work, the authors used Doubao to generate the images of flow representation of Figure 9 in this paper. After using this tool, the authors reviewed and edited the content as needed and take full responsibility for the content of the published article.

References

1. Baeyens, J.; Zhang, H.; Nie, J.; Appels, L.; Dewil, R.; Ansart, R.; Deng, Y. Reviewing the potential of bio-hydrogen production by fermentation. *Renew. Sustain. Energy Rev.* **2020**, *131*, 110023.
2. Wang, M.; Dewil, R.; Maniatis, K.; Wheeldon, J.; Tan, T.; Baeyens, J.; Fang, Y. Biomass-derived aviation fuels: Challenges and perspective. *Prog. Energy Combust. Sci.* **2019**, *74*, 31–49.
3. Lv, X.; Zhao, C.; Yan, N.; Ma, X.; Feng, S.; Shuai, L. Sustainable aviation fuel (SAF) from lignin: Pathways, catalysts, and challenges. *Bioresour. Technol.* **2025**, *419*, 132039.
4. Griffin, M.B.; Iisa, K.; Dutta, A.; Chen, X.; Wrasman, C.J.; Mukarakate, C.; Yung, M.M.; Nimlos, M.R.; Tuxworth, L.; Baucherel, X. Opening pathways for the conversion of woody biomass into sustainable aviation fuel via catalytic fast pyrolysis and hydrotreating. *Green Chem.* **2024**, *26*, 9768–9781.
5. Kumar, A.; Katahira, R.; Yang, Z.; Bayles, A.; Kumar, A.; Ruddy, D.; Bell, D.C.; Heyne, J.S.; Johnson, D.K.; Mittal, A. Advancing sustainable aviation fuel with high-energy-density bicycloalkanes production from corn stover mixed sugars. *Cell Rep. Phys. Sci.* **2025**, *67*, 102692.
6. Deng, Y.; Kong, W.; Zhang, H.; Dewil, R.; Baeyens, J. Solar Tower Continuous Saturated Steam Generation. *Lect. Notes Eletr. Engieering* **2022**, *938*, 3–11.
7. Li, S.; Kang, Q.; Baeyens, J.; Zhang, H.L.; Deng, Y.M. Hydrogen Production: State of Technology. In *IOP Conference Series: Earth and Environmental Science, Proceedings of the 10th International Conference on Environment Science and Engineering (ICESE 2020), Vienna, Austria, 18–21 May 2020*; IOP Publishing Ltd.: Bristol, UK, 2020; Volume 544.
8. *China Rural Statistical Yearbook*; China Statistics Press: Beijing, China, 2021; p. 4.
9. Jiang, D.; Hao, M.; Fu, J.; Liu, K.; Yan, X. Potential bioethanol production from sweet sorghum on marginal land in China. *J. Clean. Prod.* **2019**, *220*, 225–234.
10. Sun, Y.; Cai, W.; Chen, B.; Guo, X.; Hu, J.; Jiao, Y. Economic analysis of fuel collection, storage, and transportation in straw power generation in China. *Energy* **2017**, *132*, 194–203.
11. Cao, J.; Pang, B.; Mo, X.; Xu, F. A new model that using transfer stations for straw collection and transportation in the rural areas of China: A case of Jinghai, Tianjin. *Renew. Energy* **2016**, *99*, 911–918.
12. Shu, Y.; Wang, X.; Jia, T.; Pan, L.; Wang, Q.; Zhang, X.; Zou, J.J. Acid-catalyzed rearrangement of biomass polycyclic sesquiterpene derivatives to high-performance alkyl-adamantanes. *Chem. Eng. Sci.* **2023**, *277*, 118851.
13. Cai, H.; Brandt, A.R.; Yeh, S.; Englander, J.G.; Han, J.; Elgowainy, A.; Wang, M.Q. Well-to-Wheels Greenhouse Gas Emissions of Canadian Oil Sands Products: Implications for US Petroleum Fuels. *Environ. Sci. Technol.* **2015**, *49*, 8219–8227.
14. Sun, P.; Young, B.; Elgowainy, A.; Lu, Z.; Wang, M.; Morelli, B.; Hawkins, T. Criteria Air Pollutant and Greenhouse Gases Emissions from US Refineries Allocated to Refinery Products. *Environ. Sci. Technol.* **2019**, *53*, 6556–6569.
15. Zeng, X. Research on the Integrated Development of Comprehensive Transportation Infrastructure Construction and the National Energy Transportation Network. *Highway* **2022**, *67*, 172–180.